RIELAC
Revista de Ingeniería Electrónica, Automática y Comunicaciones

PPG & ECG Annotation Tool: Software for annotation of ECG and PPG signals

Arianna Carralero Paredes, Roger E. Rivero Labrada, Alexander A. Suárez-León, Alexander Sóñora-Mengana, Juan C. García Naranjo

ABSTRACT / RESUMEN

The study and early diagnosis of cardiac arrhythmias are of great interest today. For several years, new studies have highlighted the potential of the photoplethysmographic wave to detect these events. However, for the design and evaluation of these algorithms, it is necessary to have electrocardiographic and photoplethysmographic signals acquired simultaneously and annotated by specialists. There is low availability of annotated photoplethysmography signals for the study of arrhythmias, as well as tools that make it possible to perform analysis and annotations on these signals. This work shows the software "*PPG & ECG Annotation Tool*" for annotating electrocardiography (ECG) and photoplethysmography (PPG) records. The proposed software facilitates three main types of annotations: characteristic points, for example, R-peaks of the electrocardiogram, arrhythmic events with adjustable duration, and signal quality. The tool contains algorithms for detecting fiducial points ECG and PPG signals and enables their correction by the user. It also allows computing time intervals and heart rates in selected segments. The software is designed for medical specialists, does not require programming skills, and the user interface is simple and intuitive. The software is available for Windows and Linux platforms.

Keywords: arrhythmias, photoplethysmographic signal, software tool, annotations

El estudio y diagnóstico precoz de las arritmias cardíacas es de gran interés en la actualidad. Desde hace varios años, nuevos estudios han destacado el potencial de la onda fotopletismográfica para detectar estos eventos. Sin embargo, para el diseño y evaluación de estos algoritmos es necesario contar con señales electrocardiográficas y fotopletismográficas adquiridas simultáneamente y anotadas por especialistas. Existe una baja disponibilidad de señales de fotopletismografía anotadas para el estudio de las arritmias, así como de herramientas que permitan realizar análisis y anotaciones sobre estas señales. Este trabajo muestra el software "PPG & ECG Annotation Tool" para anotar registros de electrocardiografía (ECG) y fotopletismografía (PPG). El software propuesto facilita tres tipos principales de anotaciones: puntos característicos, por ejemplo, picos R del electrocardiograma, eventos arrítmicos con duración ajustable y calidad de la señal. La herramienta contiene algoritmos para la detección de puntos de referencia de señales ECG y PPG y permite su corrección por parte del usuario. También permite calcular intervalos de tiempo y frecuencias cardíacas en segmentos seleccionados. El software está diseñado para médicos especialistas, no requiere conocimientos de programación y la interfaz de usuario es sencilla e intuitiva. El software está disponible para plataformas Windows y Linux.

Palabras claves: arritmias, señal fotopletismográfica, herramienta de software, anotaciones.

PPG & ECG Annotation Tool: Herramienta para la anotación de señales de ECG y PPG.

1.- INTRODUCTION

One-third of the deaths globally caused by non-communicable diseases are due to cardiovascular diseases, constituting the first cause of death worldwide. Above three-quarters of CVD deaths occur in low- and middle-income countries [1]. In 2020 in Cuba, heart disease claimed the lives of about 30 thousand people, positioning it as the principal cause of death in the country. Among heart diseases, cardiac arrhythmias are common. In Cuba, arrhythmias were responsible for 921 deaths that year [2].

Recibido: 02/2023 Aceptado: 05/2023

The electrocardiogram (ECG) is the principal method and current gold standard for detecting and diagnosing arrhythmias. The ECG allows us to determine the relationships between the different segments and intervals of the signal and the alterations of the cardiac rhythm, elements that facilitate the identification of the type of arrhythmia. The study and diagnosis of arrhythmias are commonly performed with ambulatory monitoring [3]. The Holter method allows monitoring and recording of the heart's electrical activity of the patient while performing daily activities. One disadvantage of the ECG is that it requires electrodes attached to the skin. These electrodes are usually uncomfortable and might limit patient movements. Besides, due to the long monitoring time, the gel between the electrodes and the patient's skin loses conductive properties and can cause skin irritation [4].

Photoplethysmography (PPG) is a simple, non-invasive, low-cost optical monitoring technique. PPG measures fluctuations induced by cardiac activity in tissue blood volume. The photoplethysmographic waveform is made up of a pulsatile component (AC), attributed to synchronous cardiac changes in blood volume with each heartbeat, superimposed on a slowly varying baseline (DC) with low-frequency components attributed to respiration, the sympathetic nervous system, and thermoregulation [5]. PPG signal acquisition requires a single sensor and is less complex than ECG acquisition. The PPG sensor is easier to use and less sensitive to skin contact than standard ECG electrodes. These characteristics reveal PPG analysis as a promising method for investigating vascular diseases. New studies indicate the potential of the photoplethysmographic waveform to detect cardiac arrhythmias [6-9].

For the study of cardiac arrhythmias, there are several ECG databases. However, the availability of annotated PPG signals that allow such studies is limited. Physionet [10] is one of the largest sources of clinical data. In March 2022, Physionet's data repository had 17 annotated databases of ECG signals for the study of various arrhythmias. However, the number of PPG databases available in the same section until July 2022 was 5. Furthermore, the goal of such signals is the heart and respiratory rate estimation and the evaluation of wave morphology variation due to exercise stress [11-15]. Most of the studies based on PPG signals for the detection of various types of arrhythmias use proprietary databases that are not publicly available [6-9].

There are several tools for the analysis and annotation of ECG signals. For instance, [16] proposes a software tool designed and optimized for analysis of the ECG signal during the detection of arrhythmias using machine learning techniques. On the other hand, [17] proposes the open-source *WaveformECG* platform that supports analysis, visualization, and interactive annotation of ECG signals. This tool has been used in several cardiac disease studies and is available on GitHub (https://github.com/PALMS-gui/PALMS) under the CVRG project open-source repository under the Apache 2.0 license. The study in [18] present the development platform and capabilities of internet-based software tool for the purpose of user-friendly manual annotation and delineation of heartbeats in 12-lead ECG databases. Another study used the ECG analysis software Pathfinder SL for detecting atrial fibrillation in long-term ECG signals [19]. The open-source software ECGAug in [20] includes a new method that generates an augmented training set of QRST signals (individual beats or rhythm bands) with precise reference point annotations.

Up to the authors' knowledge, there are a few software tools for analyzing and marking fiducial points and the occurrence of events in the PPG signal. The study in [21] proposes a computer program for analyzing the photoplethysmographic signal recorded by PPG sensors of smart-watches or portable devices. The aim of this software is the detection of atrial fibrillation. Another study presents a software application that allows the automatic detection, visualization, and manual correction of the annotations of biomedical signals such as ECG and PPG [22]. This software features three types of manual annotations: fiducial point detection, event detection, and signal quality.

The search performed in international datasets suggests few annotated PPG signals for studying arrhythmias. Furthermore, there is a lack of software tools that allows analyzing and marking this signal. This paper proposes a software tool for annotating arrhythmia events and artifacts in electrocardiographic and photoplethysmographic signals. "PPG & ECG Annotation Tool" is a software tool with a simple and intuitive graphical interface aimed at cardiologists and medical science specialists. This tool processes both signals, i.e., ECG and PPG, in parallel. Such a feature is handy when processing recordings from multiparametric databases such as MIMIC [10].

2.- MATERIALS AND METHODS

Python 3.6.8 for Linux is the developing platform. The user interface uses *PyQt 5.9.1*. The tool requires several third-party packages like *NumPy*, *SciPy*, and *Sklearn*. *NumPy* is a base package for scientific computing with *Python* that contains functions for linear algebra, Fourier analysis, basic statistics, and others. *SciPy* is an algorithms collection from mathematics, science, and engineering based on *Python*. *Sklearn* is a library for machine learning and data analysis. *Another component is the PyQtGraph* library. *PyQtGraph* is a library for developing graphical user interfaces in data acquisition, signal processing, and analysis applications. The integrated development environment is the free version of the IntelliJ

IDEA *PyCharm 2018.2.4*. *PyCharm* is a dedicated IDE for *Python* and *Django,* which provides a wide range of essential tools for developers. Figure 1 shows the general block diagram of the software.

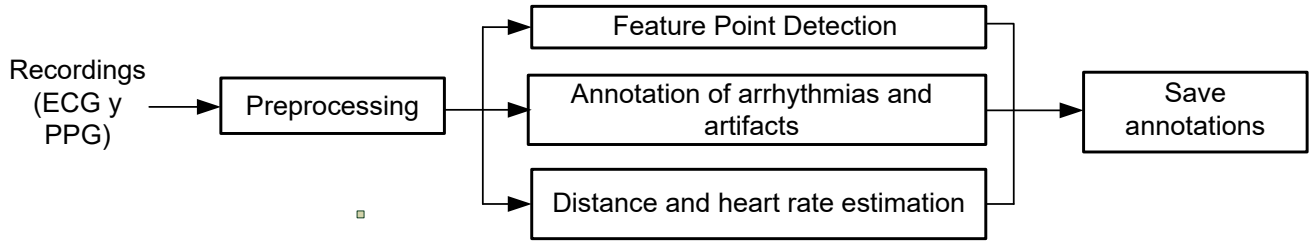

Figure 1

Block diagram of the software tool

The preprocessing block includes a fourth-order, zero-phase bandpass Butterworth filter. The cut-off frequencies for the photoplethysmographic signal are 0.5 Hz and 10 Hz, while for the electrocardiographic signal, the low cut-off frequency is 0.05 Hz, and the high cut-off frequency is 40 Hz. Once the signals are filtered, the user may perform three groups of operations: (1) fiducial points detection on both signals, (2) annotation of arrhythmia events or artifacts, and (3) the use of support tools such as measurement of time intervals and heart rate in segments chosen by the user.

The software allows the detection of the R wave peak in the ECG signal and peak, foot, and dichrotic points in the PPG signal. For the detection of R peaks, the algorithm based on thresholds of the first and second derivative of the ECG signal was used [23]. Detection of PPG signal peaks uses the method proposed in [24]. Firstly, the algorithm detects possible peaks using the derivative's method. Then, aiming to reduce the false positive rate, the algorithm filters out detected peaks using the heart's refractory period and a heuristics process. In the next step, the algorithm groups the peak candidates into clusters. The maximum amplitude within each group is the algorithm output and corresponds to a signal peak.

The method for detecting the pulse wave foot is an adaptation of the method proposed by Zhang et al. [25] to estimate the end of the T wave in ECG signals. This method uses the output of the PPG waveform peak detector algorithm. First, at each systolic peak, the algorithm searches backward for each wave where the area under the curve is maximum. The maximum area under the curve corresponds with the minimum point in the signal trace and the pulse wave foot.

The study in [26] shows a dichrotic-notch point detection algorithm that is fast and easy to implement. In this study, we implemented a variation of the method proposed in [26]. This method uses the first and second derivatives of the signal and three fundamental steps: 1) amplitude threshold search, 2) derivative slope inversion, and 3) empirical formulae. The algorithm searches candidates in the interval between one systolic peak and the foot of the next pulse wave. These points come from the two detection algorithms implemented in the tool and described above.

After the automatic fiducial points detection stage, the user can manually correct the generated annotations to ensure accuracy. The recommended workflow for the software is to: (a) apply automatic detection algorithms, (b) check the generated points, and (c) manually correct the points where necessary. In addition, the software allows annotations of 11 types of arrhythmias (*asystole*, *bradycardia*, *tachycardia*, *ventricular fibrillation*, *ventricular tachycardia*, *atrial fibrillation*, *flutter*, *isolated ventricular premature beats*, *isolated atrial premature beats*, *bigeminy,* and *trigeminy*) and of low quality in the signals, for example, due to the occurrence of artifacts. Finally, the tool allows you to save all the annotations made.

For the validation of the implemented detection algorithms, we propose the use of synthetic signals with controlled features. For this purpose, we generated twenty PPG signals using the *PPGSynth* tool [27]. *PPGSynth* allows the generation of synthetic PPG signals from a single PPG pulse pattern composed of two combined Gaussian functions. *PPGSynth* synthesizes the PPG waveform for regular heartbeats and three types of irregular heartbeats: compensation, reset, and interpolation.

Premature heartbeats change the PPG signal, causing the occurrence of irregular segments. There are two types of premature heartbeats, premature atrial contractions, and premature ventricular contractions. *PPGSynth* supports irregular PPG signals resulting from premature atrial contractions. Premature atrial contractions change the PPG waveform for two consecutive beats. Based on the difference between the duration of the first beat and the second beat, the study in [27] classifies beats into four types: compensation, reset, interpolation, and reentry. The definitions of these heartbeats are as follows:

- Compensation heartbeat: the second beat is prolonged, and the sum of the duration of the first beat and the duration of the second beat is the duration of two reference beats.
- Restart heartbeat: The second heartbeat is prolonged, but the sum of the duration of the first heartbeat and the duration of the second heartbeat is less than the duration of two reference heartbeats.
- Interpolation heartbeat: the sum of the duration of the first beat and the duration of the second beat is equal to the length of a reference beat.
- Reentry heartbeat: The sum of the duration of the first beat and the duration of the second beat is less than the duration of a reference beat.

PPGSynth includes the first three classes of irregular heartbeats and allows the generation of signals with different sampling frequencies, time durations, and noise levels. Given a type of irregular heartbeat, PPGSynth adds those heartbeats randomly in the generated interval.

The synthetic dataset for the evaluation includes 20 signals of 5 min duration with a sampling frequency of 300 Hz and a heart rate of 60 beats per minute (bpm). The generated synthetic dataset includes four groups: regular heartbeats, compensation heartbeats, reset heartbeats, and interpolation heartbeats. Each group contains five PPG signals with a different signal-to-noise ratio (SNR). The added noise is Gaussian white noise. Noise levels were selected by reference to the *Noise Stress Test Database* [10] used to assess the robustness of ECG processing algorithms. SNRs lower than 6 dB strongly affect the morphology of the PPG signal. Thus, only levels equal to or above 6 dB were used in the evaluation.

PPGSynth does not allow direct access to the fiducial points of the generated signal. Thus, we modified the application's code to store these values in a MATLAB file. The saved feet, peaks, and dichrotic points were used as a reference to evaluate the detection algorithms contained in the tool proposed in this study.

The performance evaluation of the algorithm requires computing the sensitivity (Se) and the positive predictive value (+P) using the formulae,

$$Se = \frac{TP}{TP+FN} \tag{1}$$

$$+\mathrm{P} = \frac{TP}{TP+FP}. \tag{2}$$

Where, TP -True Positive, FN -False Negative, FP -False Positive.

In this study, a point is "considered detected" -True Positive- when the algorithm's output is within a window of 66 ms around the annotation generated by the *PPGSynth* tool, or equivalently, ±10 samples at 300 Hz. When the previous condition does not hold for a given point, it will be a False Negative, i.e., the point detection fails. Furthermore, the detected point is also a False Positive since it does not correspond to any fiducial point in the signal trace.

Other metrics for evaluating performance in detection tasks are accuracy (μ) and precision (σ). In this study, we compute both of them for each record:

$$\mu = \frac{1}{N}\sum_{i=0}^{N} P_{alg} - P_{ref} \tag{3}$$

$$\sigma = \sqrt{\frac{1}{N-1}\left((P_{alg} - P_{ref}) - \mu\right)^2} \tag{4}$$

Where, P_{ref} are the positions in seconds of the points used as reference, P_{alg} are the positions in seconds of the points detected by the algorithms and N is the number of fiducial points of the PPG signal detected.

3. - RESULTS

Tables 1-3 show the evaluation results of the algorithms for detecting the foot, peak, and dichrotic points of the PPG signals. Each table contains the results of TP, FN, FP Se, +P, accuracy (μ), and precision (σ) for the four groups of signals with different SNRs. The most unfavorable results for each algorithm are in bold letters.

Table 1

Results of detecting the foot of the photoplethysmographic wave.

Rhythm type	Noise Type (SNR)	TP	FN	FP	Se	P+	μ (ms)	σ (ms)
Regular	None (∞)	303	2	1	0.99	0.99	-11.2	4.9
	Gaussian (24 dB)	300	2	1	0.99	0.99	-8.6	19.3
	Gaussian (18 dB)	296	11	11	0.96	0.96	-4.8	29.1
	Gaussian (12 dB)	245	51	51	0.83	0.83	-3.3	**33.8**
	Gaussian (6 dB)	175	125	126	**0.58**	**0.58**	3.2	**36.0**
Compensation	None (∞)	300	1	0	0.99	1	-10.7	4.6
	Gaussian (24 dB)	300	1	0	0.99	1	-5.7	20.7
	Gaussian (18 dB)	291	10	10	0.97	0.97	-7.4	27.8
	Gaussian (12 dB)	251	50	50	0.83	0.83	-3.3	**34.7**
	Gaussian (6 dB)	174	127	128	**0.58**	**0.58**	-2.7	**36.9**
Restart	None (∞)	300	1	0	0.99	1	-10.8	3.8
	Gaussian (24 dB)	301	0	0	1	1	-7.3	20.5
	Gaussian (18 dB)	284	17	17	0.94	0.94	-6.1	26.7
	Gaussian (12 dB)	235	66	66	0.78	0.78	-0.4	**34.8**
	Gaussian (6 dB)	201	100	100	**0.67**	**0.67**	-4.9	**36.8**
Interpolation	None (∞)	302	1	0	0.99	1	-10.4	4.1
	Gaussian (24 dB)	300	3	2	0.99	0.99	-10.4	19.7
	Gaussian (18 dB)	288	15	14	0.95	0.95	-4.7	28.9
	Gaussian (12 dB)	259	44	43	0.85	0.86	-5.3	**35.8**
	Gaussian (6 dB)	188	115	115	**0.62**	**0.62**	0.0	**36.6**

Table 2

Results of detecting the peak of the photoplethysmographic wave.

Rhythm type	Noise Type (SNR)	TP	FN	FP	Se	P+	μ (ms)	σ (ms)
Regular	None (∞)	304	0	0	1	1	3.3	0
	Gaussian (24 dB)	301	0	0	1	1	2.8	6.5
	Gaussian (18 dB)	306	0	1	1	0.99	3.3	11.4
	Gaussian (12 dB)	295	0	0	1	1	5.1	19.2
	Gaussian (6 dB)	291	8	9	0.97	0.97	1.4	29.4
Compensation	None (∞)	300	0	0	1	1	3.2	12.3
	Gaussian (24 dB)	300	0	0	1	1	3.6	6.0
	Gaussian (18 dB)	300	0	0	1	1	2.6	11.8
	Gaussian (12 dB)	298	2	2	0.99	0.99	1.8	19.3
	Gaussian (6 dB)	287	13	14	0.96	0.95	2.1	**30.1**
Restart	None (∞)	299	1	0	0.99	1	3.2	1.2
	Gaussian (24 dB)	301	0	0	1	1	3.6	6.0
	Gaussian (18 dB)	300	0	0	1	1	3.8	11.7
	Gaussian (12 dB)	298	2	0	0.99	1	3.4	19.6
	Gaussian (6 dB)	293	7	7	0.98	0.98	2.4	27.5
Interpolation	None (∞)	301	1	0	0.99	1	3.4	1.1
	Gaussian (24 dB)	302	0	0	1	1	3.4	5.8
	Gaussian (18 dB)	302	0	0	1	1	3.1	11.0
	Gaussian (12 dB)	300	2	2	0.99	0.99	4.2	18.6
	Gaussian (6 dB)	295	7	8	0.98	0.97	0.4	29.2

Table 3

Results of detecting the dichrotic point of the photoplethysmographic wave.

Rhythm type	Noise Type (SNR)	TP	FN	FP	Se	P+	μ (ms)	σ (ms)
Regular	None (∞)	293	12	10	0.96	0.97	6.6	11.6
	Gaussian (24 dB)	275	26	25	0.91	0.92	2.9	25.7
	Gaussian (18 dB)	263	44	44	0.86	0.86	3.4	**32.1**
	Gaussian (12 dB)	220	76	75	**0.74**	0.75	7.2	**33.0**
	Gaussian (6 dB)	210	89	90	**0.70**	**0.70**	12.6	**36.2**
Compensation	None (∞)	297	4	3	0.99	0.99	4.2	9.0
	Gaussian (24 dB)	283	18	17	0.94	0.94	0.1	28.0
	Gaussian (18 dB)	266	35	34	0.88	0.88	3.8	**32.3**
	Gaussian (12 dB)	233	68	67	0.77	0.77	8.3	**36.1**
	Gaussian (6 dB)	184	117	118	**0.61**	**0.61**	5.5	**38.3**
Restart	None (∞)	294	7	5	0.97	0.98	4.7	8.7
	Gaussian (24 dB)	270	31	30	0.89	0.90	-1.1	26.7
	Gaussian (18 dB)	264	37	36	0.88	0.88	3.7	**31.5**
	Gaussian (12 dB)	236	65	64	0.78	0.79	5.2	**34.5**
	Gaussian (6 dB)	193	108	107	**0.64**	**0.64**	4.6	**39.2**
Interpolation	None (∞)	294	9	3	0.97	0.99	4.2	9.2
	Gaussian (24 dB)	284	19	15	0.94	0.95	0.6	24.5
	Gaussian (18 dB)	265	38	35	0.87	0.88	3.3	**33.1**
	Gaussian (12 dB)	229	74	70	0.76	0.77	11.8	**33.1**
	Gaussian (6 dB)	199	104	99	**0.66**	**0.67**	9.1	**36.6**

Figure 2 shows the graphic user interface of the application, including the main menu, the toolbar, and the graphical area divided into two sections.

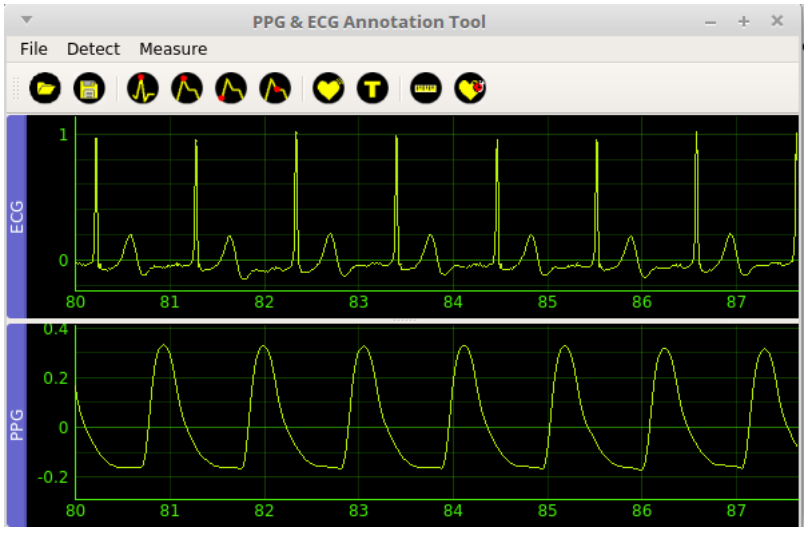

Figure 2

Main panel graphical interface (upper: ECG, lower: PPG)

The main menu and toolbar provide access to the software options. Figure 3 shows the layout of the toolbar with a description below.

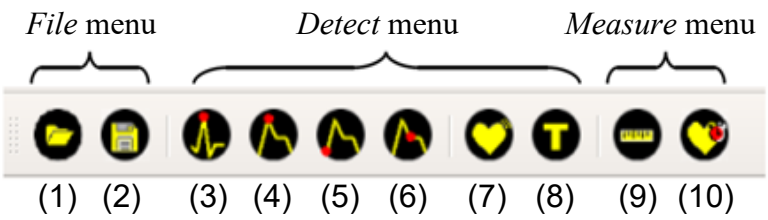

Figure *3*

Toolbar of *PPG & ECG Annotation Tool* software

The *File* menu provides the following actions: *Open, Save, and Exit.* The *Exit* option is only available in the main menu. The *Open* (1) option allows loading a *.mat* file with an ECG signal and a PPG signal. *Save* (2) allows storing the signals and the annotations made by the user in *.mat* files, Matlab's proprietary format. This action will only be available if some action is performed on the record, whether it detects characteristic points of any of the signals or labels any segment.

The *Detect* menu options are available to the user after opening a record. The actions included in this menu are (3)- *Peak R* (ECG), (4)- *Peak* (PPG), (5)-*Foot* (PPG), (6)-*Dichrotic* (PPG), (7)-*Arrhythmia* and (8)-*Type*.
Fiducial point detection actions (3)-(6) automatically detect the points in the corresponding previously filtered signal. The user can manually correct the positions of each point in case of errors after finishing the automatic detection process. For each detected point, the software displays a popup menu with three entries: *Adjust point*, *Remove point*, and *Add point*, see Figure 4. *Adjust point* allows the user moving the current point around the window, *Remove point* removes the selected point, and *Add point* adds a new point.

Figure *4*

Popup menu for the correction of the points detected by the tool.

The *Arrhythmia* (7) option in the *Detect* menu creates a sliding window that the user can place and size at will. The beginning and end of the window mark the interval that the user will subsequently classify. The *Type* (8) action is available once the user adjusts the window. This action selects the annotating mark for the corresponding segment, see Figure 5. Possible annotations marks are *Asystole*, *Bradycardia*, *Tachycardia*, *Ventricular Tachycardia*, *Ventricular Fibrillation*, *Atrial Fibrillation*, *Flutter*, *Isolated PVC*, *Isolated PAC*, *Bigeminy*, *Trigeminy*, *Low signal quality ECG*, *Low signal quality PPG.*

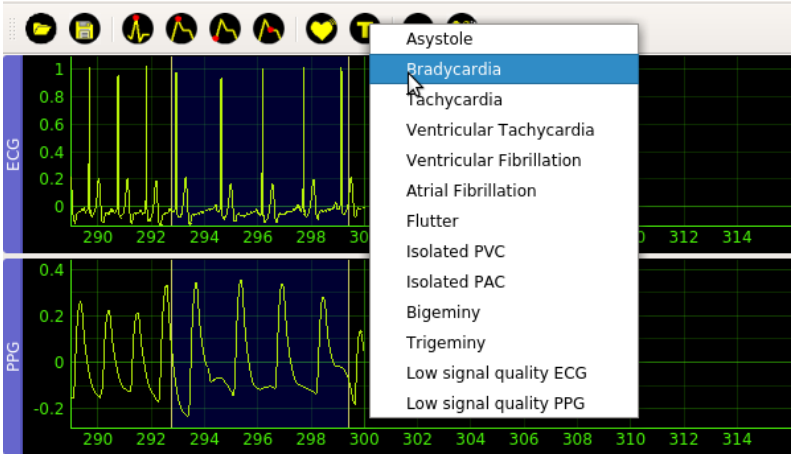

Figure *5*

Classification of a segment of the registry.

Each time the user performs segment labeling in a window, the application shows in a panel on the top-right the beginning, the ending, and the label of the current window, see Figure 6. This information panel includes a button called *Actions* that allows the user to delete selected annotations or chronologically order previously marked arrhythmias.

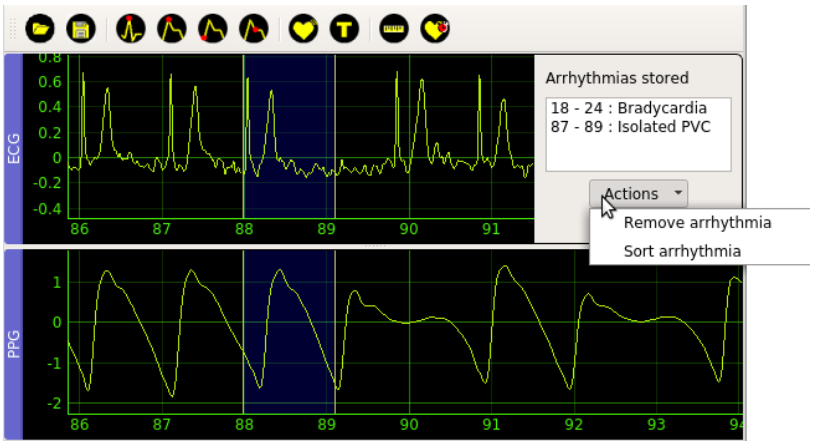

Figure *6*

Information panel with the start, end and classifications made.

The *Measure* menu provides two information tools to the user: *Distance* (9) and *Heart rate* (10). With the *Distance* option, the user can show the time interval in seconds between two points, for example, two R peaks. The *Heart rate* tool allows the calculation of the heart rate value in the selected interval. Both options show the computed values in the graphical area, see Figure 7.

Figure *7*

Estimation of the heart rate in an interval of 1 min.

4.- DISCUSSION

From the Tables 1-3, it is clear that the performance of the detection methods is almost independent of the type of rhythm. Of the three algorithms evaluated, the best results correspond to peak detection, while the most unfavorable ones belong to the dichrotic point detection algorithm. All three algorithms show a decline in sensitivity, positive predictive value, and precision as the signal-to-noise ratio worsens.

Table 1 states the algorithm output has high Se and +P for signals with high SNR, i.e., above 18 dB. In PPG signals with high SNR, the region around the foot of the photoplethysmographic wave undergoes a few variations, so the algorithm exhibits high performance. Figure 8a shows the output of the algorithm for detecting the foot of the pulse waveform using a signal with irregular compensation heartbeats and SNR of 18 dB. It is clear that in this low-noise scenario, the algorithm performs well.

When the SNR is below 18 dB, the signal morphology is compromised. The method fails when the noise incorporates fluctuations in the region close to the foot of the pulse wave because the calculation of the area under the curve, which is the indicator used for detecting the foot, is biased due to noise. Figure 8b shows a signal with irregular compensation heartbeats and SNR of 6 dB. The segment illustrates three cases where the output of the detection algorithm (+) and the reference value (o) differ by more than 10 samples (33 ms). This interval is highlighted with black dashed lines. In the three cases where the algorithm output is out for region of interest, 3 FN and 3 FP are added to the performance statistics. The figure shows how the algorithm fails when a signal fluctuation occurs to the right of the reference point; this causes the algorithm to find a minimum that does not correspond to the foot of the pulse wave. The decrease of the SNR negatively influences the algorithm's results due to the deterioration of the signal morphology.

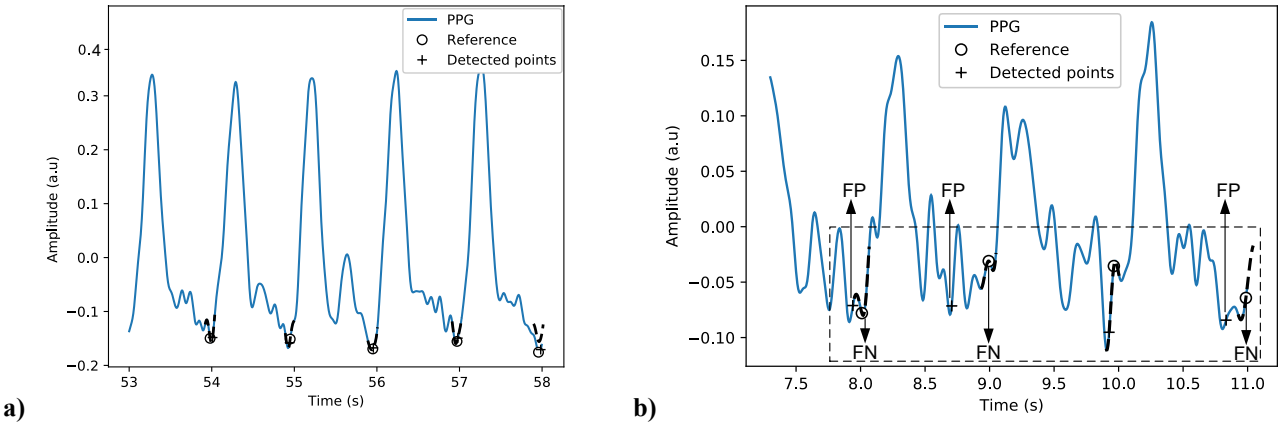

Figure 8

Detection of the beginning of the waves of the PPG signal, a) signal with irregular compensation heartbeats and SNR of 18 dB, b) signal with irregular compensation heartbeats and SNR of 6dB

The algorithm for detecting the systolic peak of the PPG signal shows better results. The main reason is that the SNR of the pulse wave peak is the largest of all the signal components. Besides, using clusters in the algorithm considerably reduces the number of FP and FN since the detection is usually more robust. However, the algorithm is also affected, although to a lesser extent, by the decrease in SNR. The algorithm fails when the noise introduces a new peak of greater amplitude in the search region. Figure 9 shows the output of the detection algorithm (+) and the reference value (o) for the signal with irregular compensation heartbeats and Gaussian white noise of 6 dB. This signal has the highest number of FP and FN in Table 2. The figure illustrates a case where the algorithm output differs by more than 10 samples from the reference.

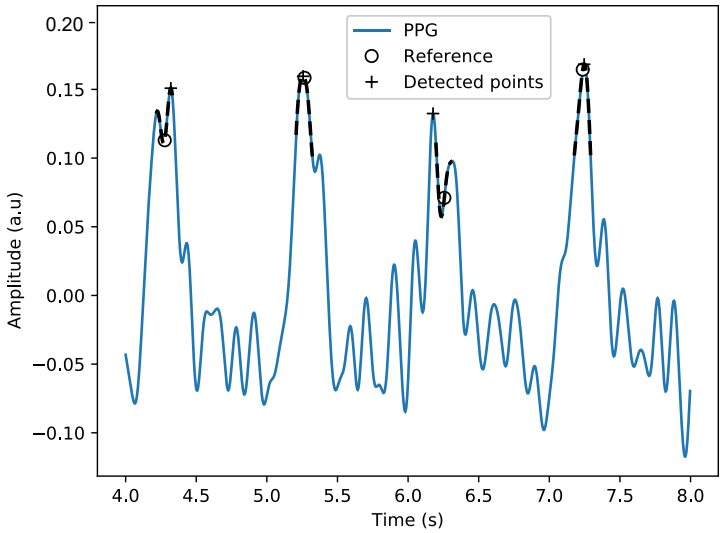

Figure 9

Detection of the systolic peak of the PPG signal

The evaluation of the algorithm for detecting the dichrotic point of the photoplethysmographic wave shows the most unfavorable results, see Table 3. This algorithm uses the derivative method, so the increase in noise levels considerably affects the detection accuracy. Figure 10 allows comparing the performance of the algorithm between two signals. As can be seen in the figure, the decrease in the signal-to-noise ratio causes noticeable variations in the morphology of the signal around the dichrotic point. These fluctuations negatively influence the result of the algorithm.

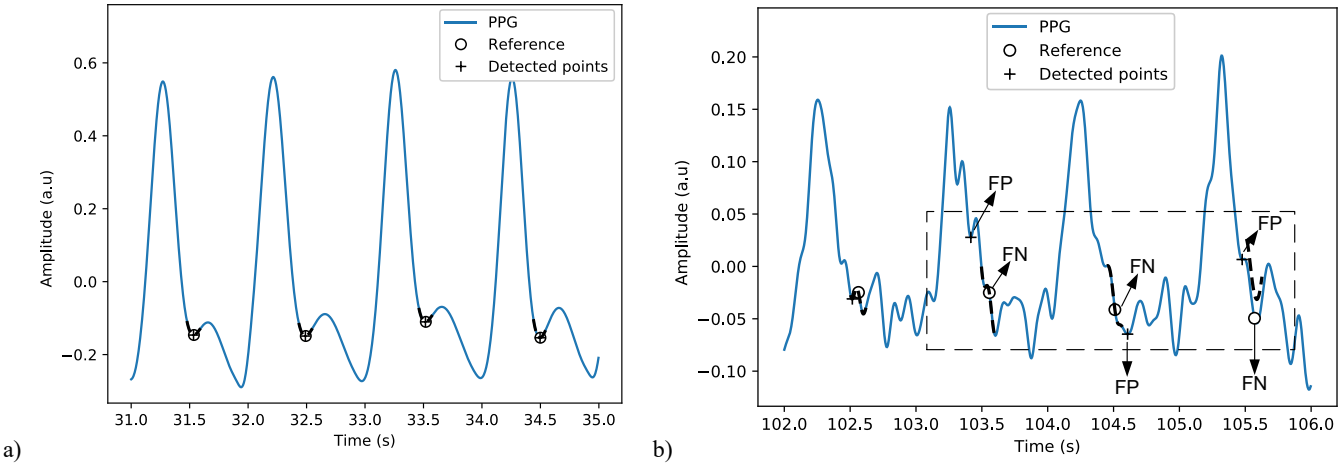

a) b)

Figure 10

Detection of the dichrotic point in the PPG signal, a) performance of the algorithm on a signal with irregular interpolation heartbeats without noise and b) signal with irregular restart heartbeats and an SNR of 6 dB.

The three evaluated algorithms show better results for signals with lower noise levels. Comparatively, the best results correspond to the systolic peak detection algorithm because the systolic peak is the most prominent fiducial point and, consequently, the easiest to detect. Moreover, the algorithm for detecting pulse wave peaks incorporates a clustering stage that allows for reducing detection errors. This stage acts as a selective filter of amplitude peaks. The detection algorithms implemented in the tool are a support method for the user. The principal purpose of these algorithms is to speed up the fiducial points annotation, so the reported performances can be considered acceptable. Although it is clear that the method performances are strongly affected by noise, a signal with low SNR, for instance, 6 dB SNR, is unsuitable for arrhythmia diagnosis because of the loss of information due to noise.

5.- CONCLUSIONS

The three evaluated algorithms show better results for signals with lower noise levels. Comparatively, the best results correspond to the systolic peak detection algorithm because the systolic peak is the most prominent fiducial point and, consequently, the easiest to detect. Moreover, the algorithm for detecting pulse wave peaks incorporates a clustering stage that allows for reducing detection errors. This stage acts as a selective filter of amplitude peaks. The detection algorithms implemented in the tool are a support method for the user. The principal purpose of these algorithms is to speed up the fiducial points annotation, so the reported performances can be considered acceptable. Although it is clear that the method performances are strongly affected by noise, a signal with low SNR, for instance, 6 dB SNR, is unsuitable for arrhythmia diagnosis because of the loss of information due to noise.

REFERENCES

1. Revueltas-Agüero M, Benítez-Martínez M, Hinojosa-Álvarez MD, Venero-Fernández S, Molina-Esquivel E, Betancourt-Bethencourt JA. Caracterización de la mortalidad por enfermedades cardiovasculares: Cuba, 2009- 2018. Revista Archivo Médico de Camagüey. 2021 Feb;25(1): 9-23.
2. Sonia Bess Constantén IAA, Elvira Sánchez Sordo, Xiomara Podadera Valdés, Miguel Ángel Martínez Morales, Isisis Alonso Expósito, Edilia Paredes Esponda. Anuario Estadístico de Salud 2020. In: Cuba MdSP, editor. 2020. Disponible en: https://salud.msp.gob.cu/wp-content/Anuario/Anuario-2020.pdf.
3. Smith Colás RE, Cobo Alea R, Vázquez Seisdedos CR. Diseño de un sistema inalámbrico de monitorización electrocardiográfica para dispositivos Android. Revista de Ingeniería Electrónica, Automática y Comunicaciones. 2020 Aug;41(2):63-79.
4. Checa V. Investigación y desarrollo de métodos para la evaluación de la calidad de señales electrocardiográficas. Tesis de Maestría. Universidad de Castilla La Mancha. 2021. Disponible en: https://ruidera.uclm.es/xmlui/bitstream/handle/10578/30445/TFM_ChecaCaballero.pdf?sequence=1&isAllowed=y.
5. Pereira T, Tran N, Gadhoumi K, Pelter MM, Do DH, Lee RJ, Colorado R, Meisel K, Hu X. Photoplethysmography based atrial fibrillation detection: a review. NPJ digital medicine. 2020 Jan 10;3(1):3.
6. Wu BF, Wu BJ, Cheng SE, Sun Y, Chung ML. Motion-robust atrial fibrillation detection based on remote-photoplethysmography. IEEE Journal of Biomedical and Health Informatics. 2023 Jun 27;(6):2705-2716.
7. Liu Z, Zhou B, Jiang Z, Chen X, Li Y, Tang M, Miao F. Multiclass Arrhythmia Detection and Classification From Photoplethysmography Signals Using a Deep Convolutional Neural Network. Journal of the American Heart Association. 2022 Apr 5;11(7):e023555.
8. Gill S, Bunting KV, Sartini C, Cardoso VR, Ghoreishi N, Uh HW, Williams JA, Suzart-Woischnik K, Banerjee A, Asselbergs FW, Eijkemans MJ. Smartphone detection of atrial fibrillation using photoplethysmography: a systematic review and meta-analysis. Heart. 2022 Oct 1;108(20):1600-7.
9. Eerikäinen LM, Bonomi AG, Schipper F, Dekker LR, de Morree HM, Vullings R, Aarts RM. Detecting atrial fibrillation and atrial flutter in daily life using photoplethysmography data. IEEE journal of biomedical and health informatics. 2019 Nov 4;24(6):1610-8.
10. Goldberger AL, Amaral LA, Glass L, Hausdorff JM, Ivanov PC, Mark RG, Mietus JE, Moody GB, Peng CK, Stanley HE. PhysioBank, PhysioToolkit, and PhysioNet: components of a new research resource for complex physiologic signals. circulation. 2000 Jun 13;101(23):e215-20.
11. Nemcova A, Vargova E, Smisek R, Marsanova L, Smital L, Vitek M. Brno University of Technology Smartphone PPG Database (BUT PPG): Annotated Dataset for PPG Quality Assessment and Heart Rate Estimation. BioMed Research International. 2021 Sep 7; 2021.

12. Pimentel MA, Johnson AE, Charlton PH, Birrenkott D, Watkinson PJ, Tarassenko L, Clifton DA. Toward a robust estimation of respiratory rate from pulse oximeters. IEEE Transactions on Biomedical Engineering. 2016 Nov 18; 64(8):1914-23.
13. Johnson AE, Pollard TJ, Shen L, Lehman LW, Feng M, Ghassemi M, Moody B, Szolovits P, Anthony Celi L, Mark RG. MIMIC-III, a freely accessible critical care database. Scientific data. 2016 May 24;3(1):1-9.
14. Moody B, Moody G, Villarroel M, Clifford G, Silva III I. Mimic-iii waveform database (version 1.0). PhysioNet. 2020;3.
15. Jarchi D, Casson AJ. Description of a database containing wrist PPG signals recorded during physical exercise with both accelerometer and gyroscope measures of motion. Data. 2016 Dec 24;2(1):1.
16. Tsoutsouras V, Azariadi D, Koliogewrgi K, Xydis S, Soudris D. Software design and optimization of ECG signal analysis and diagnosis for embedded IoT devices. Components and Services for IoT Platforms: Paving the Way for IoT Standards. 2017:299-322.
17. Winslow RL, Granite S, Jurado C. WaveformECG: A platform for visualizing, annotating, and analyzing ECG data. Computing in science & engineering. 2016 Aug 24;18(5):36-46.
18. Stoyanov T. Web-Based Software Tool for Electrocardiogram Annotation. InContemporary Methods in Bioinformatics and Biomedicine and Their Applications 2022 Mar 12 (pp. 322-331). Cham: Springer International Publishing.
19. Haeberlin A, Roten L, Schilling M, Scarcia F, Niederhauser T, Vogel R, Fuhrer J, Tanner H. Software-based detection of atrial fibrillation in long-term ECGs. Heart rhythm. 2014 Jun 1;11(6):933-8.
20. Stabenau HF, Bridge CP, Waks JW. ECGAug: A novel method of generating augmented annotated electrocardiogram QRST complexes and rhythm strips. Computers in Biology and Medicine. 2021 Jul 1;134:104408.
21. Dörr M, Nohturfft V, Brasier N, Bosshard E, Djurdjevic A, Gross S, Raichle CJ, Rhinisperger M, Stöckli R, Eckstein J. The WATCH AF trial: SmartWATCHes for detection of atrial fibrillation. JACC: Clinical Electrophysiology. 2019 Feb;5(2):199-208.
22. Fedjajevs A, Groenendaal W, Agell C, Hermeling E. Platform for analysis and labeling of medical time series. Sensors. 2020 Dec 19;20(24):7302.
23. Suarez Leon A, Varon C, Willems R, Van Huffel S, Vazques Seisdedos C. PyECG: A software tool for the analysis of the QT interval in the electrocardiogram. Revista de Ingeniería Electrónica, Automática y Comunicaciones. 2018:54-69.
24. Carralero-Paredes A, Suárez-León AA, Sóñora-Mengana A, García-Naranjo JC. Detección de arritmias a partir de la determinación de la frecuencia cardiaca con fotopletismografía. Orange Journal. 2021 Nov 23;3(5):42-52.
25. Zhang Q, Manriquez AI, Médigue C, Papelier Y, Sorine M. An algorithm for robust and efficient location of T-wave ends in electrocardiograms. IEEE Transactions on Biomedical Engineering. 2006 Nov 20;53(12):2544-52.
26. Chakraborty A, Sadhukhan D, Mitra M. Accurate detection of dichrotic notch from PPG signal for telemonitoring applications. International Journal of Biomedical Engineering and Technology. 2021;37(2):121-37.
27. Tang Q, Chen Z, Allen J, Alian A, Menon C, Ward R, Elgendi M. PPGSynth: An innovative toolbox for synthesizing regular and irregular photoplethysmography waveforms. Frontiers in Medicine. 2020 Nov 2;7:597774.

CONFLICT OF INTERESTS

Authors have no conflict of interests to declare

AUTHORS CONTRIBUTION

Arianna Carralero Paredes, review and bibliographic analysis, design and conception of the software, manuscript writing and correction, and figure design. **Alexander A. Suárez-León**, software tool conception, and design, critical review of the paper, and the methodology followed for its preparation. **Alexander Sóñora-Mengana, Juan C. García Naranjo** and **Roger E. Rivero-Labrada** contributed to the critical review of the article and the methodology followed for its preparation.

AUTHORS

Arianna Carralero Paredes, graduated of Biomedical Engineering, Master in Biomedical Engineering., Universidad de Oriente, Santiago de Cuba, Cuba, mmvd08@nauta.cu, https://orcid.org/0000-0003-1169-2375 , her research interests include biomedical signal processing.

Roger Ernesto Rivero Labrada, Engineer in Electronics, Master in Information Technology and Communications. He is with the Department of Biomedical Engineering at the Universidad de Oriente, Santiago de Cuba, Cuba, roger@uo.edu.cu, https://orcid.org/0000-0003-0372-3338 . His areas of interest include biomedical instrumentation, microcontroller systems, and biomedical signal processing and analysis

Alexander Alexeis Suárez-León, engineer in Automatics, Master, and Ph.D. in Biomedical Engineering. He is with the Department of Biomedical Engineering of the Universidad de Oriente, Santiago de Cuba, Cuba, aasl@uo.edu.cu, https://orcid.org/0000-0002-9393-4552 . His areas of interest include machine learning applications for biomedical signal processing, embedded systems, and programmable hardware.
Alexander Sóñora-Mengana, graduated of Electronic and Telecommunications Engineering, Master in Biomedical Engineering, and Ph.D. in Technical Sciences, Center for Medical Biophysics. Santiago de Cuba. Cuba, alexander.sonora@uo.edu.cu, https://orcid.org/0000-0001-7872-6758 , his research interests include signal processing and medical imaging.
Juan Carlos García Naranjo, graduate of Telecommunications Engineering, Master in Biomedical Engineering, and Ph.D. in Technical Sciences, Center for Medical Biophysics. Santiago de Cuba, Cuba, juankcanada@gmail.com, https://orcid.org/0000-0003-1649-3383 , his research interests include signal processing and medical imaging.